Desalination and Water Treatment
www.deswater.com
doi: 10.1080/19443994.2013.795876

52 (2014) 1287–1298
February

Taylor & Francis
Taylor & Francis Group

Optimal design of integrated total site utility–multi-stage flash desalination plant

M.H. Khoshgoftar Manesh[a], H. Janalizadeh[a], A.M. Blanco Marigorta[b], M. Amidpour[a,*], M.H. Hamedi[a]

[a]*Energy & Process Integration Research Center, Department of Energy Systems Engineering, Faculty of Mechanical Engineering, K.N. Toosi University of Technology, Pardis St., Mollasadra Ave., Vanak Sq., Tehran, Iran*
Tel./Fax: +98 21 88677272; email: amidpour@kntu.ac.ir
[b]*Department of Process Engineering, Universidad de Las Palmas de Gran Canaria, Edificio de Ingenierías-Tafira Baja, 35017, Las Palmas de Gran Canaria, Spain*

Received 17 December 2012; Accepted 21 March 2013

ABSTRACT

Central site utility of process industries can produce steam at different levels and the excess steam can be used to produce the desalinated water simultaneously. This paper presents the potential of total site process integration and exergoeconomic optimization to find optimal coupling between central site utility system and multi stage flash (MSF) desalination. In the first step, total site analysis has been applied to better understand the integration between site utility and MSF desalination. In this regard, the total site sink/source profiles and Site Utility Grand Composite Curves have been demonstrated to find best scenario for integration. Also, an accurate targeting procedure has been used. In the second step, exergoeconomic optimization has been applied to find optimum MSF desalination integrated with central utility. A case study is used to illustrate the usefulness of the proposed procedure to find optimum integrated MSF/site utility plant.

Keywords: Site utility; Total site; MSF desalination; Integration; Exergoeconomic; Optimization

1. Introduction

Freshwater and energy are two inseparable and essential commodities for sustaining human life on earth. Rapid population growth and industrialization, especially in developing countries in the recent past, have placed pressing demands for both fresh water and energy. Typically, desalination processes are powered by energy derived from combustion of fossil fuels which contribute to acid rain and climate change by releasing greenhouse gasses as well as several other harmful emissions [1]. Large dual-purpose plants are built to reduce the cost of electricity production and freshwater. Up to 30% of desalination cost is due to the energy requirement for the production of freshwater [2,3]. Combining desalination technologies with available heat sources is beneficial and can improve the economics of the combined processes.

Moreover, a central site utility is considered as a unit that consumes energy greatly. The main objective

*Corresponding author.

of the site utility is to produce the steam, which must satisfy the energy requirements of the site, mainly electricity, steam, mechanical power, and cooling water.

The design and optimization of site utility systems is one of the most challenging topics in process industries, as the complexity of equipment networks and choice of operating conditions present significant challenges to optimize utility systems in practice. The simulation and optimization of the utility systems require an accurate estimation of the cogeneration potential for the total site analysis as it aids the evaluation of performance and profitability of the energy systems [4]. Cogeneration targeting in utility systems is used to determine fuel consumption, shaft power production, and cooling requirements before the actual design of the utility systems [5]. To estimate cogeneration potential of the site utility system, its overall picture has to be represented in form of the site utility grand composite curve (SUGCC) [6] starting with construction of the total site profiles (TSP) [7,8].

Furthermore, thermoeconomic analyses in thermal system design are always focused on the economic objective. However, knowledge of only the economic minimum may not be sufficient in the decision-making process since solutions with higher thermodynamic efficiency, in spite of small increases in total costs, may result in much more interesting designs due to the changes in energy market prices or in energy policies.

In the field of thermoeconomics, design optimization aims at minimizing the total levelized cost of the system products, which implicitly includes thermodynamic information in the fuel cost rate through the fuel exergy flow rate. Various methodologies have been suggested in the literature as the ways for pursuing this objective based on different approaches [9–19].

The pervious researches about desalination system [1–3,9–28] focused on the dual purpose power desalination plants make use of thermal energy from power plants in the form of low-pressure steam to provide heat input to desalinations. In this paper, we focus on low grade heat of steam network of process plant to integrate with multi stage flash (MSF) desalination plant.

This paper suggested a way to perform multi-objective optimization in order to find solutions that simultaneously satisfy exergetic and economic objectives. This corresponded to a search for the set of Pareto optimal solutions with respect to the two competing objectives. Former research has focused on total site analysis or exergoeconomic optimization separately. In this paper, the integrated approach was developed for coupling MSF desalination with low grade heat of central site utility. In this regard, the cogeneration targeting method was used for estimation of fuel consumption, steam, power, and desalinated water production that is proposed by Khoshgoftar Manesh et al. [10].

The goal of this work was to find optimum coupling of MSF desalination plant with central site utility through total site analysis, an accurate cogeneration targeting, and exergoeconomic optimization.

2. System description

A typical chemical plant usually consists of several chemical production processes, which consume heat and power to make products in order to obtain maximum profit (Fig. 1). The heat and power are supplied by a site utility system. The site utility system consumes fuel in boilers, supplies the necessary steam to chemical processes via several steam mains, and produces power via steam turbines. The processes may also generate steam at various levels. The steam generated by processes can be supplied to the steam mains, and eventually consumed in other processes.

The design procedure for evaluation of integration of desalination technologies with an existing site utility system is shown in Fig. 1. The characteristics of site utility, such as available heat load at temperatures for use in desalination, are obtained from total site analysis [8,9]. Computer code is used to obtain the performance indicators, for example, GOR and exergoeconomic parameters, for desalination technology.

The performance indicators from computer code are fed to the total site to determine the energy savings and electricity demand obtained by heat upgrade options. Integration of desalination system affects cooling utility and electricity demand. This demand change is evaluated from total site and grand utility composite curves.

3. Modeling

3.1. MSF desalination

Fig. 2 demonstrates the MSF desalination plant. The plant includes evaporators in heat recovery section and deaerator and brine heater in heat rejection section. Some of cooling sea water joins intake seawater and some of it enters the deaerator. The intake seawater enters to heat rejection section after adding cooling seawater. The cooling seawater is the output of heat rejection section.

Brine recycle from last effect of heat rejection section enters the condenser tubes' heat recovery section. The output of condenser tubes enters to brine

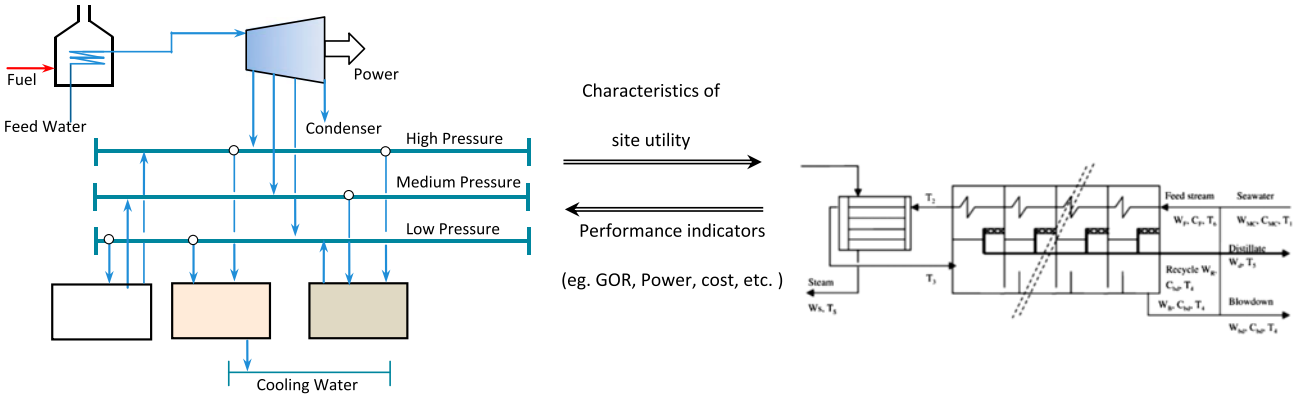

Fig. 1. Schematic of coupling of an MSF plant and site utility.

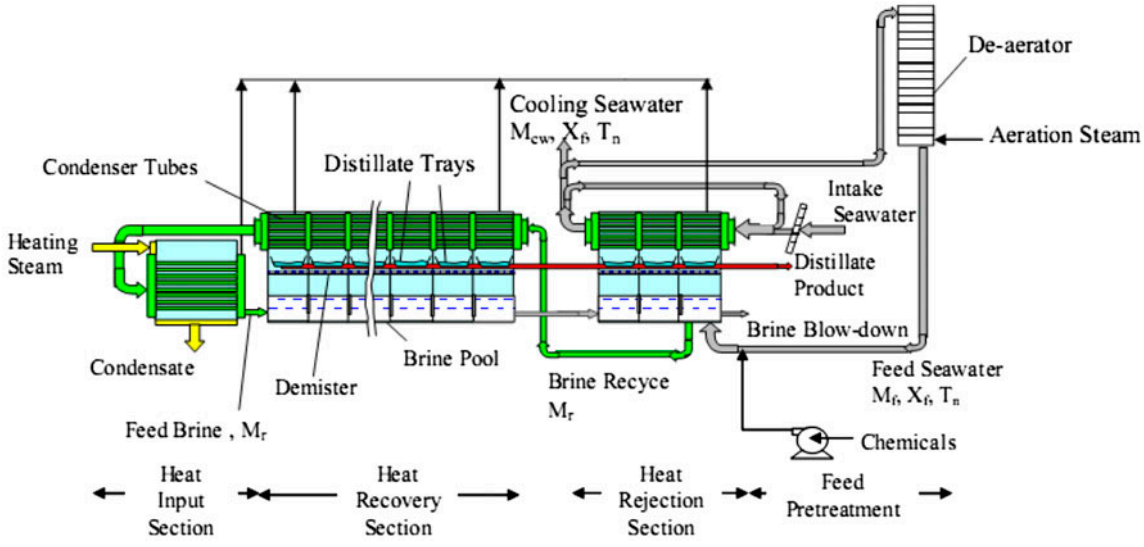

Fig. 2. Schematic of thermal vapor compression desalination (MSF).

heater and is heated by heating steam. The temperature of feed brine at the first stage of heat recovery section is called top brine temperature.

For evaluation of thermal performance and heat transfer area of system, the models developed by Alasfour et al. [14], Shakib et al. [15], and Bin Amer [16] have been applied. The mass and energy balances and the heat transfer equations for evaporators, jet ejectors, and end condensers have been developed. These model equations can be simulated to determine the values of GOR.

The following assumptions are considered for desalination system:

- Vapor formed in each effect is free of salt.
- Thermal loss from desalination to environmental is negligible.
- Final reject salinity is assumed 70,000 ppm.
- Heat transfer area of evaporators 2 to N is the same.
- Initially, it was supposed that the temperature difference of all effects is the same where T_1 and T_N are first and last effect temperature, respectively.

Mass and salinity balance equations for all the effects, the condenser, and the distillate tank are given by Eqs. (1)–(5), as shown in Table 1. Also, the exergy balance equations given by Eqs. (6)–(10) are presented in Table 1. Heat transfer area, heat transfer coefficient, and logarithmic mean temperature difference equations can be obtained by using Eqs. (11)–(17) as shown in Table 2. The temperature profile equations to determine the saturated vapor temperature, vapor condensation temperature, brine temperature, and nonequilibrium allowance are presented in Table 3.

Table 1
Mass and energy balance and exergy equations

Equations	Descriptions	
$W_r = \frac{W_s \times \lambda}{C_p \times (\Delta T + \alpha)}$	Mass balance equation between recycled stream and steam	1
$W_d = \frac{W_r \times C_p \times (T_3 - T_4)}{\lambda_{ave}}$	Mass balance equation between recycled stream and desalinated stream	2
$W_b = \frac{W_d \times x_f}{(x_b - x_f)}$	Mass balance equation between desalinated stream and brine	3
$W_f = W_b + W_d$	Mass balance equation between desalinated stream and brine and feed	4
$GOR = \frac{W_d}{W_s}$	Gain Output Ratio definition	5
$e_{che} = -N_m \times R \times T_0[(x_w \times \ln x_w) + (x_s \times \ln x_s)]$	chemical exergy	6
$e_{phy} = C_p(T - T_0) - T_0 \times [(C_p \times \ln(\frac{T}{T_0})) - \frac{P - P_0}{T_0 \times \rho_m}]$	physical exergy	7
$\rho_m = N_m\left(\frac{(\rho_w + \rho_s)}{(\rho_s \times \rho_f)}\right)$	Density of mixture	8
$e_{fuel} = e_{pump} + e_{steaminput} + e_{brineinput}$	the exergy of fuel input definition	9
$e_{product} = e_{desalinated}$	the exergy of product output definition	10

Table 2
Heat transfer area, heat transfer coefficient, and logarithmic mean temperature difference equations

Equations	Descriptions	
$A_1 = \frac{M_s L_s}{U_{e_1}(T_s - T_1)}$	Heat transfer area of effect 1	11
$A_i = \frac{(D_{i-1} + D_{i-1})L_{i-1}}{U_{e_i}\Delta T}$	Heat transfer area of effects 2 to n	12
$A_{tot} = \sum_{i=1}^{n} A_i$	Total heat transfer area of effects	13
$A_c = \frac{(D_N + D_N)L_N}{U_c LMTD_c}$	Heat transfer area of condenser	14
$U_e = 1.9695 + 1.2057 \times 10^{-2} \times T_b 8.5989 \times 10^{-5} \times T_b^2 + 2.5651 \times 10^{-7} \times T_b^3$	overall heat transfer coefficients in the evaporator [13]	15
$U_c = 1.7194 + 3.2063 \times 10^{-3} \times T_V + 1.5971 \times 10^{-5} \times T_V^2 - 1.9918 \times 10^{-7} \times T_V^3$	overall heat transfer coefficients in the condenser [13]	16
$LMTD_c = (T_f - T_{cw})/\left(\ln \frac{T_N - T_{cw}}{T_N - T_f}\right)$	Logarithmic mean temperature difference of condenser	17

3.3. Central site utility

Two main components in the proposed site unity system have been considered:

3.3.1. Modeling of steam turbine

Thermodynamic model was used to estimate the steam turbine's isentropic efficiency as follows [29]:

$$\eta_{is} = \frac{W_{max}}{W_{is,max}} \tag{18}$$

$$W_{max} = \frac{W_{is,max} - A}{B} \tag{19}$$

where A and B are constants that depend on the turbine and are functions of the saturation temperature. A and B are calculated by Eqs. (20) and (21), respectively.

$$A = a_0 + a_1 \Delta T_{sat} \tag{20}$$

$$B = a_2 + a_3 \Delta T_{sat} \tag{21}$$

The values of these constants are given in Table 4.

3.3.2. Modeling of boiler

The steam boilers can be modeled in two alternative ways—with a constant efficiency model or with a

Table 3
Temperature profile equations

Equations	Descriptions	
$\Delta T = \frac{T_3 - T_4}{N}$	Temperature difference of all effects (initial assumption)	18
$T_3 = T_s - 3$	Temperature of effect 1 (top brine temperature)	19
$T_i + 1 = T_i + \Delta T$	Temperature of effects 2 to N	20
$T_f = T_N + \Delta T \times N$	Feed seawater temperature	21
	Temperature of the vapor	22
$T_{v_{i-1}} = T_i - \mathrm{BPE}_i$		
$T_i = T_i + \mathrm{NEA}_i(T)$	Temperature of the vapor formed by flashing	23
$\mathrm{BPE} = Ax + Bx^2 + Cx^3$	Boiling point elevation	24
$A = 8.325 \times 10^{-2} + 1.883 \times 10^{-4}T + 4.02 \times 10^{-6}T^2$		
$B = -7.625 \times 10^{-4} + 9.02 \times 10^{-5}T - 5.2 \times 10^{-7}T^2$		
$C = 1.522 \times 10^{-4} - 3 \times 10^{-6}T - 3 \times 10^{-8}T^2$		
$\mathrm{NEA}_i = 0.33\frac{(T_{i-1} - T_i)^{0.55}}{T_{v_i}}$	Nonequilibrium allowance	25

Table 4
The regression coefficients used in the isentropic efficiency equation

	Back pressure turbines		Condensing turbines	
	$W_{max} \leqslant 2000$kW	$W_{max} > 2000$kW	$W_{max} \leqslant 2000$kW	$W_{max} > 2000$kW
a_0 (kW)	0	0	0	–463
a_1 (kW/℃)	1.08	4.23	0.662	3.53
a_2	1.097	1.155	1.191	1.22
a_3 (℃$^{-1}$)	0.00172	0.000538	0.000759	0.000148

variable efficiency model; however, in reality the boiler efficiency varies significantly with the load.

Varbanov [30] defined a modified version of the boiler model, formulated by Shang [31]:

$$Q_{BF} = \Delta h_{gen}[(b_{Blr} + 1)m_{stm} + a_{Blr}m_{stm,max}] + R_{BD}m_{stm}\Delta h_{pre} \quad (22)$$

This model allows the from the boiler blow down to be accounted for separately from the other losses. The particular values of the performance coefficients for this model, referenced by Shang [31], are $a = 0.0126$ and $b = 0.2156$.

The boiler efficiency represents the fraction of the fuel heat used to generate the useful steam:

$$\eta_{Blr} = \frac{Q_{stm}}{Q_{BF}} \quad (23)$$

4. Methodology

4.1. Process integration techniques

4.1.1. Total site analysis

In this section, the proposed model was presented in detail to target the cogeneration potential for site utility systems. The procedure uses the SUGCC, which represents another form of the site composite curves [2]. The SUGCC was obtained from the site composite curves by being represented on temperature–enthalpy axes of each steam main by its saturation temperature and steam generation and usage loads, respectively, from the source and sinks profiles of the site composites. The differences between steam generation and steam usage set the VHP demand or the supply heat available at each main.

This model calculates the minimum required flow rate from a steam generation unit and the levels of superheat in each steam main based on the heat loads

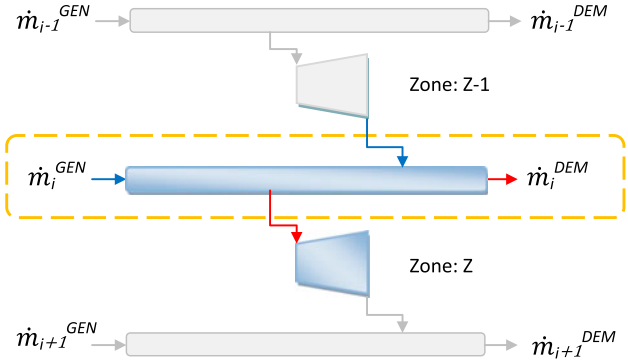

Fig. 3. Mass load balance for i-th steam main.

specified by SUGCC [32,33]. Fig. 3 shows a schematic of the utility system layout. The given L steam mains are indexed by i from the highest pressure steam main, meaning that i is equal to 1, 2, 3, and 4 for very high pressure (VHP), high pressure (HP), medium pressure (MP), and low pressure (LP) steam mains, respectively. There is an expansion zone between two steam mains. Each zone is indexed by Z starting from top, i.e. $Z=1$ is for VHP–HP, and one single steam turbine is placed in each zone.

4.1.2. Application of targeting

To calculate the header condition and to estimate cogeneration targets, the developed targeting strategy has been applied. In this regard, at the boiler exit, for a given pressure and steam temperature, the enthalpy can be obtained with the aid of steam tables. The actual input enthalpy of steam mains are usually provided from the calculations of the previous steam mains. The input isentropic enthalpy of steam main can be obtained in the superheated region. Then, the efficiency is calculated. The actual enthalpy which will serve as the input enthalpy for the next zone is then calculated using the isentropic enthalpies and efficiency by Eq. (24).

$$h_{\mathrm{i,actual}} = h_{\mathrm{i-1,isentropic}} - \eta(h_{\mathrm{i-1,isentropic}} - h_{\mathrm{i,isentropic}}) \tag{24}$$

In this study, the calculation of superheat temperature at each steam level was done using the iterative procedure based on a certain desirable amount of superheat in the LP steam main. This superheat was required to be set at 10–20℃ [9]. If the degree of superheat in the resulting LP steam main was less than the required level, then operating conditions of VHP would be updated and iterated until the acceptable superheated conditions would be met for the LP steam main [32,33].

The mass flow rate of steam expanding through the Zth turbine ($\dot{m}_z$) can be calculated by the mass balance for ith by Eq. (25), as shown in Fig. 3 [10].

$$\dot{m}z = \dot{m}_{z-1} + \dot{m}_{i-1}^{\mathrm{DEM}} - \dot{m}_{i-1}^{\mathrm{GEN}} \tag{25}$$

where $\dot{m}_i^{\mathrm{GEN}}$ is the flow rate of steam generated by the process and $\dot{m}_i^{\mathrm{DEM}}$ is the flow rate of steam demanded by the process, which can be calculated by Eqs. (26) and (27), respectively:

$$\dot{m}_i^{\mathrm{DEM}} = \frac{\dot{Q}_i^{\mathrm{DEM}}}{h_i^{\mathrm{Actual}} - h_{f,i}} \tag{26}$$

$$\dot{m}_i^{\mathrm{GEN}} = \frac{\dot{Q}_i^{\mathrm{GEN}}}{h_i^{\mathrm{Actual}} - h_{f,i}} \tag{27}$$

where $h_{f,i}$ = the enthalpy of the saturated liquid enthalpy at the pressure of ith steam main.

4.2. Thermoeconomic modeling

Thermoeconomic is the branch of engineering that combines exergy analysis and economic principles to provide the system designer or operator with information not available through conventional energy analysis and economic evaluations but crucial to the design and operation of a cost effective system [34,35].

The governing equation of thermoeconomic model for the cost balancing of an energy system is written as:

$$C_{\mathrm{F}} + Z = C_{\mathrm{P}} \tag{28}$$

By defining exergy cost of each stream, c, Eq. (28) could be changed to:

$$c_{\mathrm{F}}E_{\mathrm{F}} + Z = c_{\mathrm{P}}E_{\mathrm{P}} \tag{29}$$

Table 5
Equation of cost of the process unit

Purchase cost equations	Descriptions	
$Z_{\mathrm{BrineHeater}} = 491 \times Q \times 1600 \times \Delta T_t^{-.7} \times \Delta P_t^{-.8} \times \Delta P_{\mathrm{s}}^{-.4}$	Price of brine heater	30
$Z_{\mathrm{MSF}} = 433.44 \times Q \times 3900 \times \Delta T_n^{-.75} \times \Delta T_t^{-.5} \times \Delta P_t^{-.1}$	Price of MSF unit	31

The above relations are global cost balance equation, which should be applied for different component. Here, for each component of combined system, cost balance equation is taken into account.

In order to perform the economic analysis, the purchase cost of equipment must be determined. The purchase cost of the MSF desalination is determined by some correlations that are proposed by El-sayed [35] (Table 5 and Eqs. (30)–(31)).

The amortization cost for a particular plant component may be written as [35,36]:

$$\mathrm{PW} = C_i - S_n \mathrm{PWF}(i, n) \tag{30}$$

$$\dot{C}\left(\frac{\$}{\mathrm{year}}\right) = \mathrm{PW} \times \mathrm{CRF}(i, n) \tag{31}$$

The present worth of the component is converted to annualized cost by using the capital recovery factor CRF (i, n), i.e. [34]. The maintenance cost is taken into consideration through the factor $\Phi = 1.05$ k for each plant component whose expected life is assumed to be 20 years [34].

4.3. Optimization

4.3.1. Multi-objective genetic algorithm

The multi-objective exergoeconomic optimization approach is applied to find optimum solution. The two issues in multi-objective optimization include: (1) finding solutions close to the true Pareto optimal set and (2) finding solutions that are widely different from each other in order to cover the entire Pareto optimal set as well as not introduce bias towards any particular objective [37–40]. Fig. 4 illustrates the scheme for the multi-objective evolutionary algorithm used in the present work. In this paper, multi-objective Genetic Algorithm has been applied for to find optimum solution.

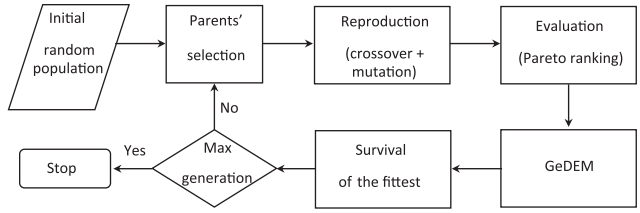

Fig. 4. Scheme for the multi-objective evolutionary algorithm used in the present work.

4.3.2. Objective functions

The two objective functions of the multi-criteria optimization problem are GOR (to be maximized) and the total cost rate of desalinated water (to be minimized)

The objective functions are as follows:

(1) Maximum GOR
(2) Minimum cost of desalinated water production (Cw)

4.3.3. Parameters

The decision variables and constrains of the optimization problem has been demonstrated in Table 6.

Table 6
Decision variables and constrains of the optimization problem for desalination plant

Discretion	Parameter	Unit	Value
Heating steam temperature	T_s	℃	60–110
Top brine temperature	TBT	℃	57–107
Salinity of seawater	x_{cw}	Ppm	36,000
Salinity of last effect brine	x_N	Ppm	50,000–70,000
Steam mass flow rate	W_s	kg/s	19
Desalinated water mass flow rate	W_d	kg/s	27.356–155
Brine mass flow rate	W_b	kg/s	446.754–319.11
Temperature of seawater	T_{cw}	℃	25
Outlet condenser temperature of seawater	T_f	℃	5℃ lower than T_N
Number of effects	N	–	6–38
Pressure of seawater	P_{cw}	Kpa	101
Tube diameter	D_t	Mm	19.05
Tube length	L_t	M	5

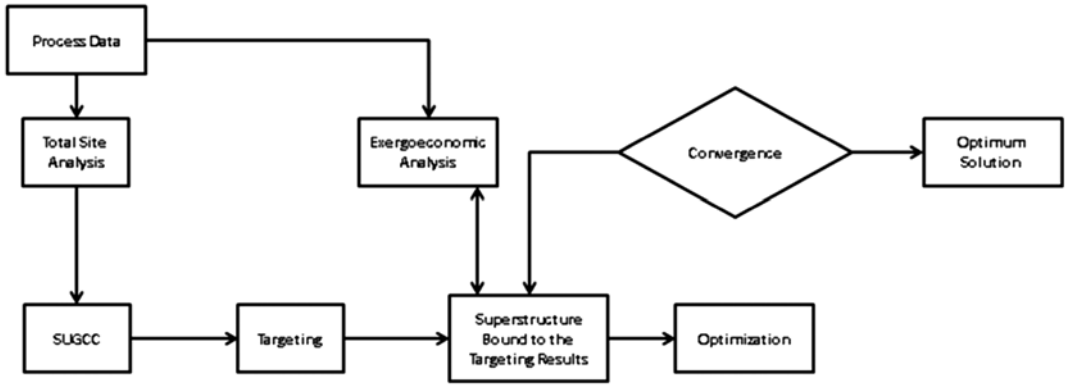

Fig. 5. Algorithm for finding optimum solution.

4.4. Procedure

The proposed procedure to find optimum coupling between site utility and MSF desalination system has been demonstrated in Fig. 5. This procedure is based on using total site analyses, an accurate cogeneration targeting method, and exergoeconomic optimization.

As shown in Fig. 5, the following steps should be considered.

Step 1: Data collection approaches for the total site analysis [10], [32,33].

Step 2: Total site analysis: From the collected data, the process source/sink profiles and the utility profiles can be plotted. A computer code developed here can produce TSP representing the heating and cooling requirements of the site. This allows targets to be set for fuel consumption in the boilers, cogeneration potential, and energy costs. Profiles can be based on either the full heat recovery data or more simply from the data for the utility exchangers only. Cogeneration potential can be targeted [10].

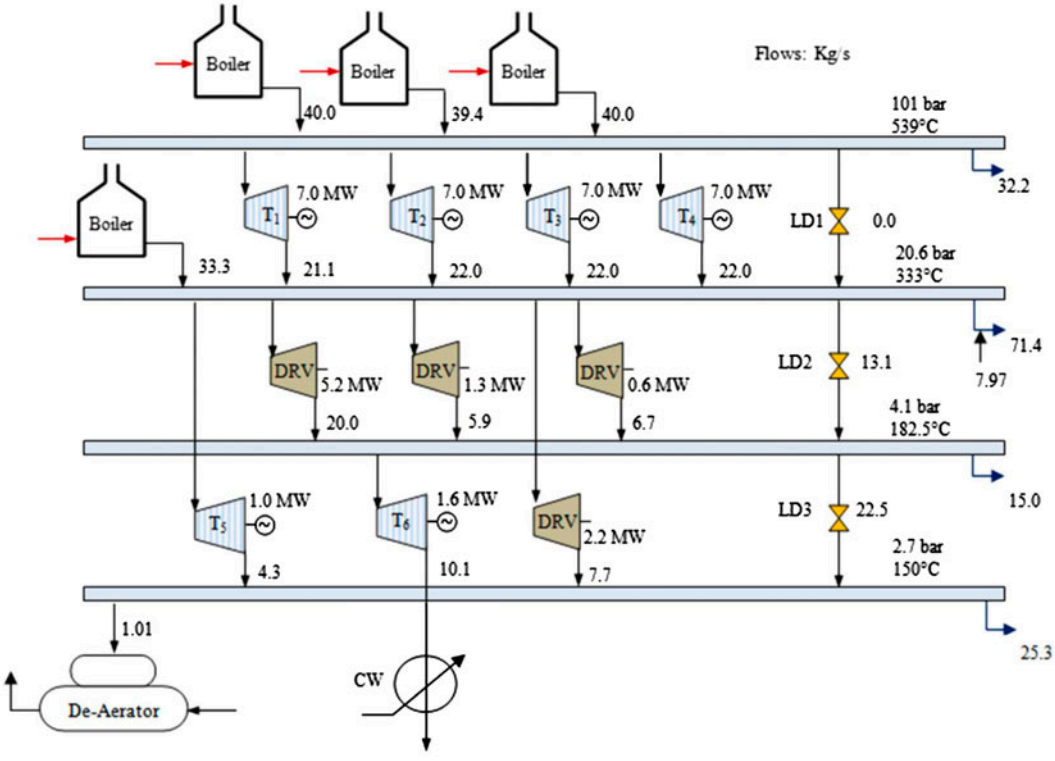

Fig. 6. Base case design [33].

Table 7
Process steam generation and usage (central site utility)

Level	Process steam generation (MW)	Process steam usage (MW)	Net heat load of process (MW)
VHP	0	110.8	110.8
HP	120	141.4	21.4
MP	47.7	57	9.3
LP	15.4	89	73.6

Step 3: Exergoeconomic analysis: Quantitative balances of the exergy and exergetic cost for each component and for the whole system are carefully considered. The exergoeconomic model, which represents the productive structure of the considered system, is used to visualize the cost formation process and the productive interaction between the components. The costs of all flows in production structure can be calculated by solving a set of equation including thermoeconomic modeling of each component [37–40].

Step 4: SUGCC: The SUGCC is obtained from the site composite curves by being represented on the temperature–enthalpy axes of each steam main by its saturation temperature, steam generation, and usages loads, respectively, from the source and sink profiles of the site composites. The area enclosed by the profile is proportional to the potential cogeneration/shaft power. The site pinch is represented by zero enthalpy between two or more steam temperature levels [10], [32,33].

Step 5: Targeting cogeneration potential: A computer code developed here can set energy targets and select utilities for individual processes. Application of these tools allows the picture of the total site to be built up from the individual processes. These tools include the composite curves, grand composite curve, and problem table which enable the engineer to predict hot and cold utility targets for individual processes. Also, the low grade heat can be identified for coupling with MSF desalination plant [10], [32,33].

Step 6: Reduced superstructure based on targeting results

Step 7: Exergoeconomic optimization coupled plant (site utility + MSF desalination). The multi-objective exergoeconomic optimization is performed in order to find optimum MSF/site utility system [37–40].

5. Case study

The proposed optimization model is applied to a site utility which was presented by Aguillar (Fig. 6) [33], which consists of four back-pressure turbines between VHP and HP levels and one back-pressure turbine between HP and LP steam levels. Two multistage turbines are available for the expansion of steam between HP–MP and MP–LP, respectively, while there are four mechanical pumps to be driven by either steam turbines or electric motors, and an electric motor is used for the supply of the feed water to the boiler.

Also, site data for heat load, electricity demands, pump electricity demand, condensate return, and cooling water is shown in Table 7 [4].

6. Results

The grand composite curves (GCC) of the individual process are modified by removing the pockets corresponding to additional heat recovery within the process. These modified process GCC are then combined together to form the total site sink and source profile Fig. 7. The SUGCC represents the horizontal separation between the source and the sink. Net heat load of process at VHP, HP, MP, and LP levels are 110.8, 21.4, 9.3, and 73.6 MW, respectively (Table 8). In addition, the potential of power production is repre-

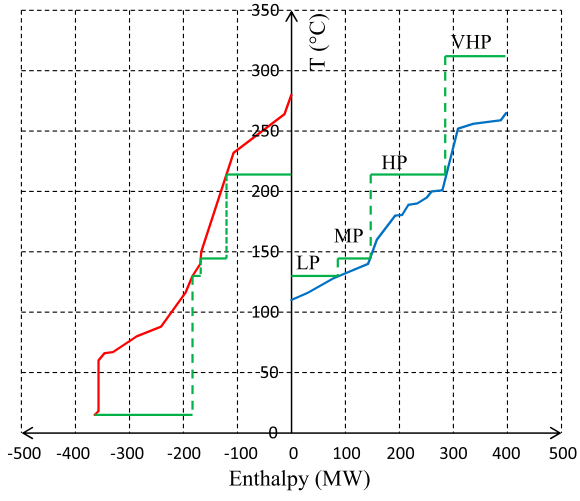

Fig. 7. Site source and sink composite curve.

Table 8
Optimum parameters values obtained by proposed method

Discretion	Parameters	Units	Optimal design
Temperature of steam	T_s	℃	101.15
Number of stages	N	–	21
Gain output ratio	GOR	–	7.59
Cost of fuel	c_{fuel}	$/MJ	3.2693
Cost of power	C_P	$/KW h	0.03
Cost of water	$c_{desalinated}$	$/m^3	0.26
Top brine temperature	TBT	℃	98.149
Mass flow of desalinated water	W_d	kg/s	155
Mass flow of brine	W_b	kg/s	319.11
Salinity of last effect brine	x_N	ppm	70,000

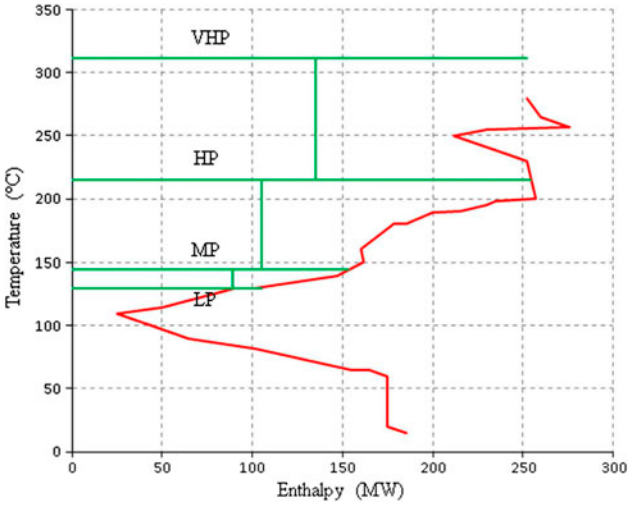

Fig. 8. Site utility grand composite curve (SUGCC).

sented as areas in the SUGCC with VHP–HP, HP–MP, and MP–LP cogeneration potential of 79.8, 58.4, and 49.1 MW as demonstrated in Fig. 8. The power generation potential is represented as areas in SUGCC with VHP–HP, HP–MP, and MP-LP cogeneration potential of 79.8, 58.4, and 49.1 MW when a full steam recovery is made within the site utility systems.

The multi-objective optimization has been performed to find the optimum solution based on the steam supply from site utility. Also, the optimum parameters obtained by multi-objective optimization for MSF desalination have been shown in Table 8. The desalinated water production in optimum integrated plant is 155 kg/s and the optimum GOR is 7.6. In addition, the optimum number of stage is 21 and the optimum flow of the brine is 319.11 kg/s. Moreover, the cost of desalinated water production is 0.26 $/m^3.

Results shows that integration of the MSF with site utility and using low grade heat of site utility is very good scenario to production of desalinated water. Also, the cost of water production is very low due to using low grade heat.

7. Conclusion

This present study demonstrated the potential of process integration techniques and exergoeconomic optimization to find optimal coupling between central site utility system and MSF desalination. In this regard, total site analysis has been applied to better understand the integration between site utility and MSF desalination. In this regard, the total site analyses and cogeneration targeting method have been performed to find best scenario for integration. In addition, exergoeconomic optimization has been applied to find optimum MSF desalination integrated with central utility. Results shows that integrated MSF-site utility is very good option to produce desalinated water through low grade heat in central site utility.

Finally, there are some suggestions to decreased exergy cost of steam supplied to MSF. By using low grade heat of site utility, the exergy cost of steam supplied to MSF decreased. Also, when the mass flow rate of LP steam increased, the exergy cost of steam supplied to MSF decreased. Furthermore, when the heat recovery of total site increased, the cost of steam decreased. However, the power generation potential decreased. In this regard, optimum heat recovery can be found to satisfy the total site demands with minimum exergy cost of products (desalinated water/process steams/power).

Nomenclature

A_c	M^2	condenser heat transfer area
W_d	kg/s	rejected mass flow rate
C_p	kJ/kg℃	specific heat capacity
W_b	kg/s	distillated mass flow rate
W_f	kg/s	feed mass flow rate of each effect
W_r	kg/s	recycled mass flow rate
W_s	kg/s	motive steam mass flow rate
λ	kJ/kg	latent heat
λ_{ave}	kJ/kg	average latent heat of the steam
$LMTD_c$	℃	condenser log mean temperature difference
T_f	℃	feed water temperature
T_{cw}	℃	cooling water temperature
T_s	℃	heating steam temperature
T_v	℃	vapor temperature
U_c	kw/m^2 ° C	overall heat transfer coefficient at condenser
U_e	kw/m^2 ° C	overall heat transfer coefficient at evaporator
X	ppm	salinity
ΔT ΔT_{cond}	℃	temperature difference
A	kg/m^2 s pa	membrane pure water permeability
B	kg/m^2 s	membrane salts permeability

Acknowledgment

The authors would like to acknowledge the Ministry of Science Research and Technology of Islamic Republic of Iran for financial supports.

References

[1] V.G. Gude, N. Nirmalakhandan, S. Deng, Renewable and sustainable approaches for desalination, Renew. Sustain. Energy Rev. 14 (2010) 2641–2654.
[2] M. Busch, W.E. Mickols, Reducing energy consumption in seawater desalination, Desalination 165 (2004) 299–312.
[3] S. Kalogirou, Effect of fuel cost on the price of desalination water: A case for renewables, Desalination 138 (2001) 137–144.
[4] A. Kapil, I. Bulatov, R. Smith, J. Kim, Site-wide low-grade heat recovery with a new cogeneration targeting method, Chem. Eng Res. Des. 90(5) (2012) 677–689.
[5] M. Sorin, A. Hammache, A new thermodynamic model for shaftwork targeting on total sites, Appl. Therm. Eng. 25 (2005) 961–972.
[6] K. Raissi, Total site integration. PhD Thesis, The University of Manchester, Manchester, UK, 1994.
[7] V.R. Dhole, B. Linnhoff, Total site targets for fuel, co-generation, emissions, and cooling, Comput. Chem. Eng. 17 (1993) S101–S109.
[8] J. Klemes, V.R. Dhole, K. Raissi, S.J. Perry, L. Puigjaner, Targeting and design methodology for reduction of fuel power and CO2 on total sites, Appl. Therm. Eng. 17(8–10) (1997) 993–1003.
[9] R. Smith, Chemical Process Design and Integration, Wiley, West Sussex, 2005.
[10] M.H. Khoshgoftar Manesh, H. Ghalami, M. Amidpour, M.H. Hamedi, A new targeting method for combined heat, power and desalinated water production in total site, Desalination 307 (2012) 51–60.
[11] M. Li, Reducing specific energy consumption in Reverse Osmosis (RO) water desalination: An analysis from first principles, Desalination 276 (2011) 128–138.
[12] M.H. Khoshgoftar Manesh, M. Amidpour, Multi-objective thermoeconomic optimization of coupling MSF desalination with PWR nuclear power plant through evolutionary algorithms, Desalination 249(3) (2009) 1332–1344.
[13] H.T. El-Dessouky, H.M. Ettouney, Fundamentals of Salt Water Desalination, Elsevier, Amsterdam, 2002.
[14] F.N. Alasfour, M.A. Darwish, A.O. Bin Amer, Thermal analysis of ME-TVC+MEE desalination system, Desalination 174 (2005) 39–61.
[15] S.E. Shakib, M. Amidpour, C. Aghanajafi, Simulation and optimization of multi effect desalination coupled to a gas turbine plant with HRSG consideration, Desalination 285 (2012) 366–376.
[16] A.O. Bin Amer, Development and optimization of ME-TVC desalination system, Desalination 249 (2009) 1315–1331.
[17] N.M. Al-Najem, M.A. Darwish, F.A. Youssef, Thermo-vapor compression desalination: Energy and availability analysis of single and multi-effect systems, Desalination 110 (1997) 223–238.
[18] F. Al-Juwayhel, H.T. El-Dessouky, H.M. Ettouney, Analysis of single-effect evaporator desalination systems combined with vapor compression heat pumps, Desalination 114 (1997) 253–275.
[19] R.B. Power, SteamJet Ejector for the Process Industries, McGrawHill, NewYork, 1994.
[20] C. Fritzmann, J. Löwenberg, T. Wintgens, T. Melin, State-of-the-art of reverse osmosis desalination, Desalination 216 (2007) 1–76.
[21] F. Vince, F. Marechal, E. Aoustin, P. Breant, Multi objective optimization of RO desalination plants, Desalination 222 (2008) 96–118.
[22] Y.Y. Lu, Y.D. Hu, X.L. Zhang, L.Y. Wu, Q.Z. Liu, Optimum design of reverse osmosis system under different feed concentration and product specification, J. Membr. Sci. 287 (2007) 219–229.
[23] T. Kaghazchi, M. Mehri, R.M. Takht, A. Kargari, A mathematical modeling of two industrial seawater desalination plants, Desalination 252 (2010) 135–142.
[24] N. Bouzayani, N. Galanis, J. Orfi, Thermodynamic analysis ofcombined electric power generation and water desalination plants, Appl. Therm. Eng. 29 (2009) 624–633.
[25] J.A. Redondo, A. Casanas, Designing seawater RO for clean and fouling RO feed: desalination experiences with the filmtec SW30HR-380 and SW30HR-320 elements—technical economic review, Desalination 134 (2001) 83–92.
[26] J.A. Redondo, I. Lanzarote, A new concept for two pass SWRO at low O & M cost using the new high-flow FILMTEC SW30–380, Desalination 138 (2001) 231–236.
[27] H.J. Oh, T.M. Hwang, S. Lee, A simplified simulation model of RO systems for seawater desalination, Desalination 238(1–3) (2001) 128–139.
[28] D. Akgul, M. Çakmakcı, N. Kayaalp, I. Koyuncu, Cost analysis of seawater desalination with reverse osmosis in Turkey, Desalination 220 (2008) 123–131, 1–3.

[29] P.S. Varbanov, S. Doyle, R. Smith, Modelling and optimization of utility systems, Chem. Eng. Res Des. 82(5) (2004) 561–578.
[30] P. S. Varbanov, Optimisation and Synthesis of Process Utility Systems, PhD Thesis, Department of Process Integration, UMIST, Manchester, UK, 2004.
[31] Z. Shang, Analysis and Optimisation of Total Site Utility Systems. PhD Thesis, UMIST, UK, 2000.
[32] M.H. Khoshgoftar Manesh, S. Khamis Abadi, M. Amidpour, M.H. Hamedi, A new targeting method for estimation of cogeneration potential and total annualized cost in process industries, Chem. Eng. Res. Des. (2013), doi: 10.1016/j.cherd.2012.12.002
[33] M.H. Khoshgoftar Manesh, M. Amidpour, S. Khamis Abadi, M.H. Hamedi, A new cogeneration targeting procedure for total site utility system, Appl. Therm. Eng. 54(1) (2013) 272–280. http://dx.doi.org/10.1016/j.applthermaleng.2013.01.043.
[34] A. Bejan, G. Tsatsaronis, M. Moran, Thermal Design and Optimization, Wiley, New York, 1996.
[35] Y.M. EI-Sayed, The Thermoeconomics of Energy Conversions, Elsevier, Amsterdam, 2003.
[36] O. Aguillar, Design and Optimisation Of Flexible Utility Systems. PhD Thesis, The University of Manchester, 2005.
[37] A. Toffolo, A. Lazzaretto, Evolutionary algorithms for multi-objective energetic and economic optimization in thermal system design, Energy 27 (2002) 549–567.
[38] G. Tsatsaronis, Thermoeconomic analysis and optimization of energy system, Prog. Energy Combust. Sci. 19 (1993) 227–257.
[39] C. Koch, F. Cziesla, G. Tsatsaronis, Optimization of combined cycle power plants using evolutionary algorithms, Chem. Eng. Process 46 (2007) 1151–1159.
[40] M.H. Khoshgoftar Manesh, M. Amidpour, M.H. Hamedi, Optimization of the coupling of PWR power plant and multi stage flash desalination plant by evolutionary algorithms and thermoeconomic method, Int. J. Energy Res. 33 (2009) 77–99.